Journal of Physics: Conference
Series

PAPER • OPEN ACCESS

Flow Fluctuation during Flow Boiling of Binary Mixtures in High Aspect Ratio Microchannel

To cite this article: Arif Widyatama *et al* 2023 *J. Phys.: Conf. Ser.* **2643** 012018

Flow Fluctuation during Flow Boiling of Binary Mixtures in High Aspect Ratio Microchannel

Arif Widyatama[1,2] ,Mandi Venter[3], Muhammad Sofwan Bin Mohamad[4], Jacob Dirker[3], Daniel Orejon[1], Khellil Sefiane[1,*].
[1]Institute for Multiscale Thermofluids, School of Engineering, University of Edinburgh, James Clerk Maxwell Building, The King's Buildings, Edinburgh EH9 3FD, UK
[2]Department of Mechanical & Industrial Engineering, Faculty of Engineering, Gadjah Mada University, Jalan Grafika No.2, Yogyakarta, 55281, Indonesia
[3]Faculty of Engineering, University of Pretoria, Lynnwood Road, Hatfield, 0028, Pretoria, SA
[4]Faculty of Mechanical Engineering & Technology, Universiti Malaysia Perlis, Pauh Putra Campus, 02600 Arau, Perlis, Malaysia

*k.sefiane@ed.ac.uk

Abstract. Flow boiling performance is affected by several factors, such as channel characteristics and working fluid types. It is found that there is still limited study that discusses the use of binary mixtures combined with high aspect ratio microchannels. The aim of this study is to investigate the flow fluctuation during flow boiling of binary mixtures in rectangular microchannels. Here, a 6 mm width and 0.3 mm depth rectangular channel was utilised, and it represents a hydraulic diameter of 571 μm and an aspect ratio of 20. In the present works, a mass flux of 10 kg m^{-2} s^{-1} was used, and the heat flux ranged from 15.2 and 21.0 kW m^{-2}. The image processing technique was applied to track the bubble tail movement. In addition, the thermal camera was utilised to gather the wall temperature distribution of the channel. The preliminary results show that the use of binary mixtures influences the vapour fraction in the channel and the flow fluctuation characteristics. Some differences are observed in terms of wall temperature characteristics. However, the rapid increase of wall temperature is found in the outlet region for high flux cases under all liquid types which suggests the dominance of dry out event.

1. Introduction

The development of the thermal management system in recent decades has triggered extensive research on flow boiling in mini/microscale. The recent review articles [1]–[5] have stressed critical aspects that need to be discussed, such as the clear definition of flow pattern, critical heat flux factors, flow instability criteria, and surface characteristics. Hence, an in-depth understanding of these areas is essentially needed.

The optimisation of the heat transfer performance of the compact thermal management system can be achieved in several ways. Surface modification is one of the popular approaches. Equally important, liquid property modification, by substance addition to the pure liquid, is believed can improve heat transfer performance. Peng et al. [6] suggested that heat transfer performance enhancement would be found by utilising a binary mixture under optimum concentration. Sitar and Golobic [7] found that the use of water-butanol mixtures can postpone the occurrence of dry-out. The study of Yang et al. [8] on the flow boiling of NH_3 water mixtures revealed that the improvement of the heat transfer coefficient was caused by the presence of nucleation due to the lower boiling point of the mixtures compared to the pure liquid. These findings show the potential of the application of binary mixtures in the boiling application, and further studies that cover various operating conditions should be conducted.

The aim of the present study is to investigate the flow boiling behaviour under different types of working fluid. Here, water, 5% v/v water-ethanol, and 5% v/v water-butanol were used as the working fluid. A high width-to-height aspect ratio rectangular channel was used with a hydraulic diameter of 571 μm. The heat flux applied in the study varied between 15.2 and 21.0 kW m^{-2}. The study first discusses the bubble tail movement. It is followed by the analysis of wall temperature under various working fluids and heat flux.

2. Research Methodology

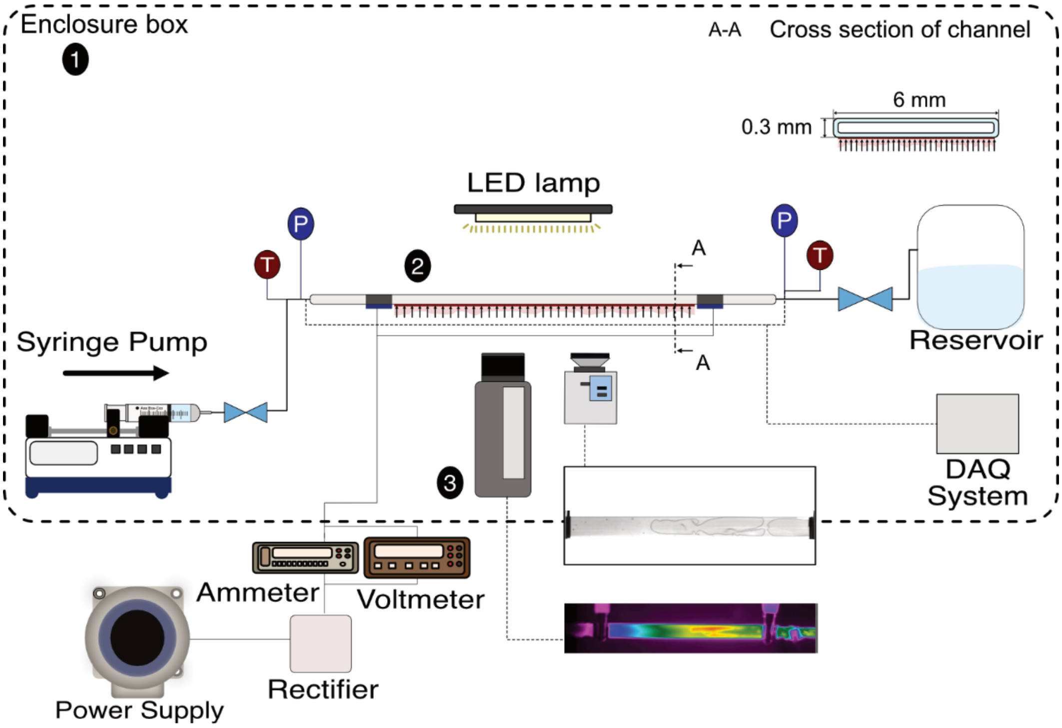

Figure 1. Experimental set up

Figure 1 depicts the experimental set up used in the present work. A detailed explanation of this set-up can be found in Widyatama et al. [9]. The liquid was circulated to the flow path by a syringe pump that was combined with a 100 ml Fortuna Optima Syringe. A glass reservoir was installed to store the used liquid which passed the main test section. It should be noted that the system was supported with the rotary table that allowed the change of flow orientation to be done. However, in the present works, the horizontal flow configuration became the main focus of the study.

A rectangular microchannel, 0.3 mm depth and 6 mm inner depth was chosen as the test section. This geometry represents an aspect ratio of 20 and a hydraulic diameter of 571 μm. The transparent heating method, as used in previous studies [10], [11] , was applied to produce one-side heating. It is achieved by adding a thin tantalum layer which provides thermal resistance. A 240 V power supply was to supply the power to the system. It is coupled with two multimeters to monitor the voltage and the current.

The wall temperature distribution was recorded by FLIR A645sc thermal camera under 25 fps setting. It had 640 x 480 resolution which allowed the entire channel to be captured. In addition, the Basler video camera (500 fps) was utilised to record the flow visualisation. In the inlet and outlet region, K-type thermocouple and pressure transducer were installed to monitor the flow condition. The signal was received by National Instrument data acquisition system and transferred to the computer which processes the data through LabView Software.

Three types of working fluid were utilised: pure water, 5% v/v water-ethanol mixtures, and 5% v/v water-butanol mixtures. The mass flux was set on 10 kg m^{-2} s^{-1}. The heat flux was varied from 15.2 – 21.0 kW m^{-2}. Since there is no pre heat applied to the liquid, the inlet temperature is similar with the environment temperature, 23.5° (± 1.5 °C)

3. Data Reduction

The mass flux, G, was determined by following equation.

$$G=\frac{\dot{V}\rho_L}{A_\mathrm{c}} \tag{1}$$

where $\dot{V}$ denotes the volumetric flow rate of the pump, ρ_L is the liquid density, and A_c is the channel internal cross-sectional area. The heat flux was converted from the input power by following equation (2)

$$q=\frac{\phi Q_\mathrm{input}}{A_\mathrm{w,in}} \tag{2}$$

where ϕ represents the heat transfer efficiency, Q_input denotes the power input, $A_\mathrm{w,in}$ is the inner channel surface area. The heat transfer efficiency was determined by considering the heat loss during the single-phase system. The details calculation can be found in [12].

The thermal camera measured the outer wall temperature of the channel. Here, the Biot number, *Bi*, should be assessed to check the temperature distribution within the channel depth. The equation (3) is used to calculate the Biot number.

$$Bi=\frac{hd}{k_\mathrm{ch}} \tag{3}$$

Where h is the heat transfer coefficient [13], d describes the channel depth, and k_{ch} is the thermal conductivity of the channel. Based on the applied test cases, a small value of Biot number was found (Bi<<1). Hence, the temperature gradient along the channel depth can be neglected. Next, several uncertainties need to be determined in the present work. The calculation was conducted based on the approach of Taylor [14]. Table 1 shows the uncertainties for the present study.

Table 1. The summary of uncertainties

Properties	Unit	Uncertainty
Pump volumetric flow rate ($\dot{V}$)	ml/hour	0.5 %
Thermocouple temperature ($T_{\text{liq,in}}$, $T_{\text{liq,out}}$)	°C	0.2 °C
IR camera measured temperature (T_{w})	°C	2 °C
Hydraulic diameter (D_{h})	mm	4 %
Inlet and outlet pressure (P_{in} , P_{out})	mbar	0.25%
Current (I)	mA	0.2 %
Voltage (U)	V	0.01 %
Heat flux (q)	W m^{-2}	6.2 %
Mass flux (G)	kg m^{-1} s^{-2}	4.1 %
Vapour quality (x)	-	8.5 %
Local liquid temperature ($T_{\text{liq,z}}$)	°C	10.37%
Heat transfer coefficient (h)	W m^{-2} K^{-1}	9.8 %
Bubble tail position (Z_{tail})	mm	11.2%

4. Result and Discussion

During flow boiling, flow fluctuation can be easily encountered, especially under low mass flux. To characterise this fluctuation, the bubble tail position, Z_{tail} , was tracked by image processing to produce further quantitative analysis. The bubble tail was measured from the inlet position, as shown in Figure 2 (a). The result of the time series measurement for the cases of water, 5% v/v water-ethanol, and 5% v/v water-butanol. The increase of heat flux, for all cases, triggers the increase of flow fluctuation as indicated by bubble tail position movement.

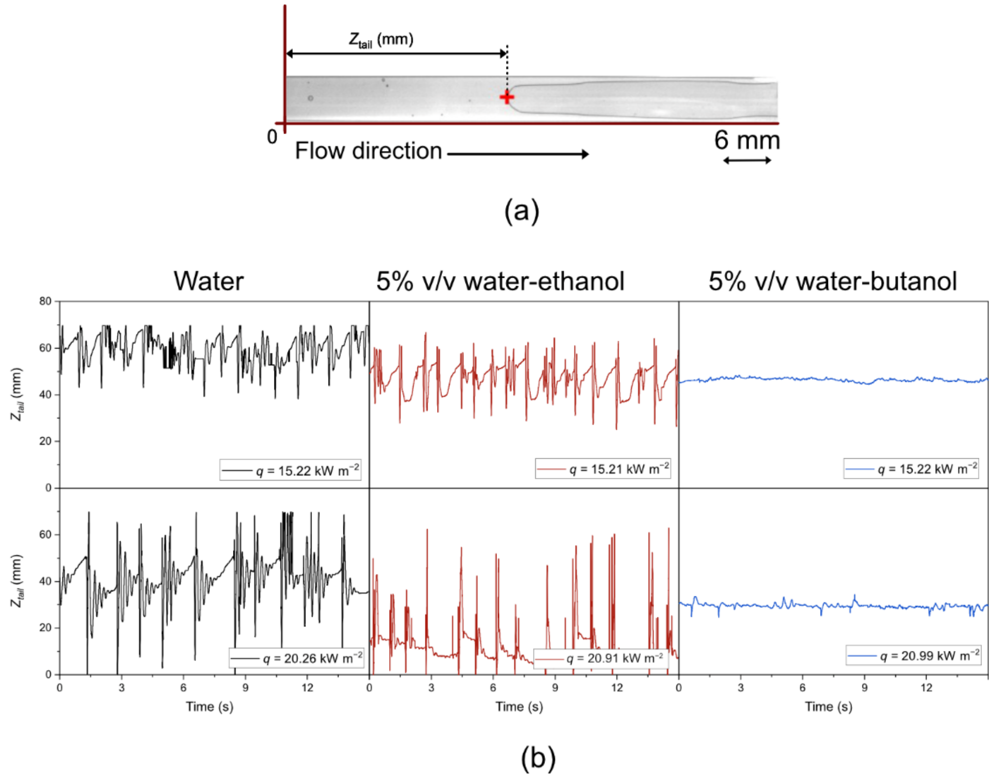

Figure 2. a) The snapshot of the flow visualisation during flow boiling. b) Time series data of flow fluctuation for water, 5% v/v water-ethanol, and 5% v/v water-butanol

Based on the time series data of the bubble tail position, the average value of the bubble tail position is determined to obtain the general characteristics during flow boiling. Figure 3 (a) shows the average bubble tail position under different types of fluids. It should be noted that due to the slight difference in channel heated length, a non-dimensional value is utilised by dividing the average bubble tail position by the channel heated length and it is set as the horizontal axis of the figure. As illustrated by a snapshot inside the figure, the non-dimensional bubble tail of 1 suggests that the channel is fully occupied by the liquid, whilst the value of zero indicates that the vapour phase dominates the channel.

Close observation of the water cases reveals that as the heat flux increases, the bubble tail position is closer to the inlet position. This trend implies that the vapour fraction in the channel becomes dominant. The increase in heat flux accelerates the liquid-vapour process phase change process. Due to the low mass flux used in the present study, the vapour phase stayed in the channel and occupied the outlet area. Furthermore, the 5% v/v water-ethanol and 5% v/v water-butanol show a slightly lower bubble tail position value than the water case. This may be due to a slight decrease in the boiling point of the mixtures caused by the addition of ethanol and butanol.

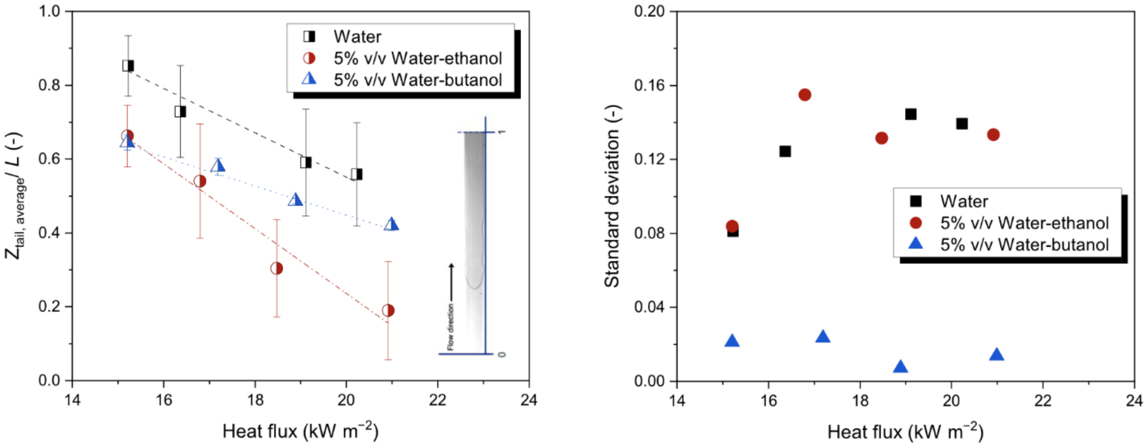

(a) (b)

Figure 3. a) The nondimensional average bubble tail position and b) the standard deviation of average bubble tail position under different heat flux for the case of water, 5% v/v water-ethanol and 5% v/v water butanol.

Another important aspect captured in the study is the standard deviation represented by the line through the points in Figure 3 (a) and independently shown Figure 3 (b). The higher deviation represents a severe bubble tail movement, as shown in the Figure 2 b. In the water cases, the flow tends to be stable in the low heat flux since the standard deviation is low. As the heat flux increases, more nucleation site is activated in the channel. This phenomenon is also found by [15] This nucleation process can trigger flow reversal. In addition, the interfacial waves in the liquid vapour interface also contribute to flow instability. While the 5% v/v water-ethanol cases show almost similar behaviour with the water cases, it is interesting to note that the 5% v/v water butanol cases produce a more stable flow, as represented by the low standard deviation shown in the Figure 3 (b). This behaviour can be caused by thermos capillary effect that is found in the self-rewetting mixtures, which allow the liquid to penetrate between the vapour and heated wall and reduce the flow fluctuation.

Figure 4 shows the wall temperature distribution along the channel for the case of water with a mass flux of 10 kg m^{-2} s^{-1} for the heat flux between 15.22 to 20.23 kW m^{-2}. The measurement point is represented by the symbol and the grey area shows the deviation, which occurs by temperature fluctuation during the period. The figure shows that for the lowest heat flux cases, q = 15.22 kW m^{-2}, the inlet and outlet area show the linear increase trend of wall temperature mainly caused by the single-phase heat transfer in the region. A slight deviation is also found in this region. In the outlet region, a slight deviation increase can be observed due to the flow fluctuation. As the heat flux increases, it is found that severe temperature fluctuation takes place during the flow boiling. This phenomenon is clearly captured in the case of 15.22 kW m^{-2}. A temperature deviation of 12.3 ºC is found at z = 63.7 mm. The temperature fluctuation also occurs closer to the inlet due to the higher vapour dominant phase in the channel.

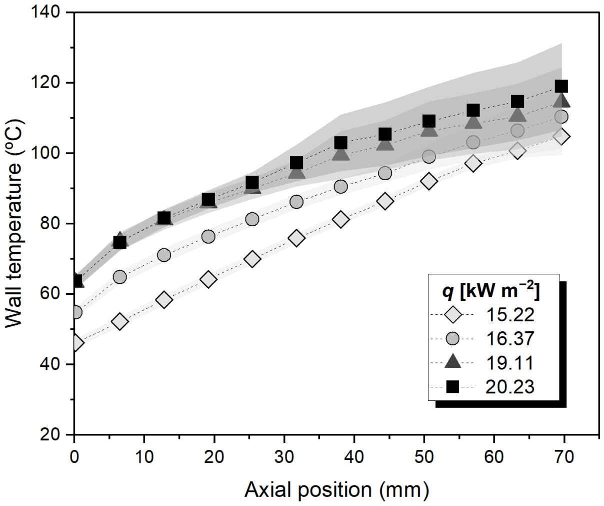

Figure 4. Wall temperature distribution for water cases under different heat flux

The wall temperature fluctuation in the Figure 4 can be associated with the flow fluctuation captured by bubble fluctuation as shown in Figure 2. In the lowest case, the bubble fluctuation tends to be stable and only produces small fluctuations. The increases in heat flux trigger the occurrence of bubble nucleation and flow instability in the channel. It directly influences the wall temperature profile. The presence of dry-out also causes the sudden increase in wall temperature.

Figure 5 depicts the distribution of wall temperature under binary mixtures of 5% v/v water-ethanol (Figure 5 (a)) and 5% v/v water-butanol (Figure 5 (b)). Close observation of the figure reveals that the additive of a small amount of methanol and ethanol influences the wall temperature distribution of the channel. For the cases of 5% v/v water-ethanol mixtures, a higher deviation is found, and it represents the more severe wall temperature fluctuation compared to pure water cases. Due to the addition of a more volatile substance in the form of ethanol, spontaneous dry-out occurs more frequently. It should be noted that the flow instability also triggers the rapid movement of the liquid phase that provides cooling to the channel. In the high heat flux cases, wall temperature fluctuation also occurs in areas close to the inlet where the liquid single phase is dominant. This phenomenon can be ascribed to the liquid mixing caused by flow reversal during flow boiling. Moving to the 5% v/v water butanol cases, the low flow fluctuation observed in Figure 2 influences the wall temperature deviation, as shown in Figure 5 b. A small number of flow reversals causes the wall temperature, particularly in the inlet and middle region, to tend to be stable with low deviation. In the outlet area of the high heat flux case, the sudden jump in wall temperature is observed as a sign of the dry out of the channel. Overall, although the flow fluctuation influences the temperature deviation, there is no significant difference in the average value of wall temperature in the outlet area. It is due to the rapid liquid-vapour phase change that triggers the dry out in this region.

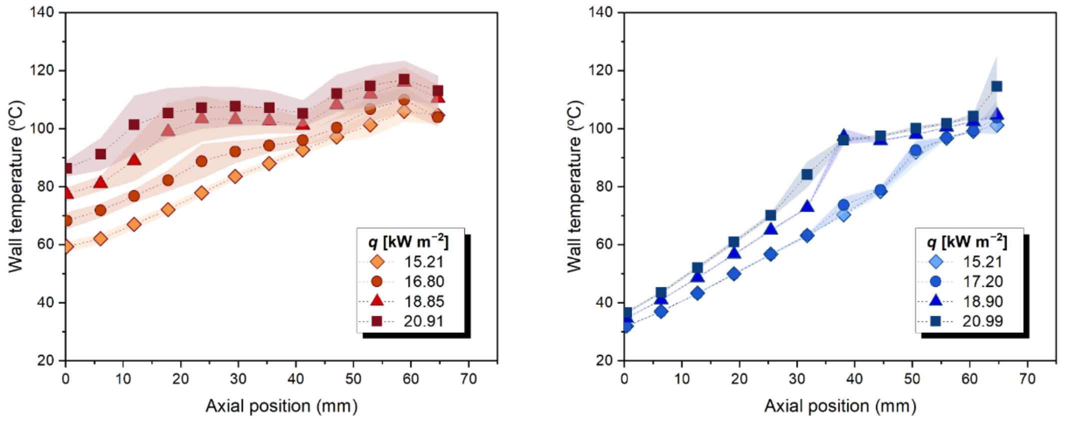

(a) (b)

Figure 5. Wall temperature distribution under different heat flux a) 5% v/v water-ethanol b) 5% v/v water-butanol

5. Conclusion

The flow boiling of binary mixtures in a high aspect ratio microchannel was experimentally investigated. Three different types of fluid were used: pure water, 5% v/v water-ethanol, and 5% v/v water butanol. The study reveals that 5% v/v water-butanol produces the most stable flow, represented by the lowest bubble tail position fluctuation. In addition, the 5% v/v water-ethanol case shows the highest vapour fraction in the channel. Regarding thermal characteristics, the deviation of wall temperature is strongly affected by flow fluctuation. In terms of wall temperature characteristics, the preliminary results suggest that slight difference is found associated with the flow fluctuation. In addition, there is no significant difference in average wall temperature in the outlet region due to the occurrence of dry-out.

Acknowledgements

The authors would like to thank the Scottish Microelectronics Centre (SMC) for the coating process of the microchannel. A.W. acknowledges Indonesia Endowment Fund for Education (Lembaga Pengelola Dana Pendidikan-LPDP), Ministry of Finance Republic of Indonesia, for the financial support.

List of References

[1] Mahmoud M M, Karayiannis T G 2016 *Exp. Therm. Fluid Sci.* **70** 270-82
[2] Cheng L, Xia G 2017 *Int. J. Heat Mass Transfer* **108** 97-127
[3] Balasubramanian K R, Peter R J, Krishnan R A 2022 *Microfluid Nanofluid* **26(10)** 80
[4] Ribatski G 2013 *Exp. Heat Transfer* **26(2-3)** 198-246
[5] Thome J R 2006 *Heat Transfer Eng.* **27(9)** 4-19
[6] Peng X F, Peterson G P, Wang B X 1996 *Int. J. Heat Mass Transfer* **39(6)** 1257-64
[7] Sitar A, Golobic I 2015 *Int. J. Heat Mass Transfer* **81** 198-206
[8] Yang R, Wang Y, Li Y 2021 *Int. J. Heat Mass Transfer* **171** 121091
[9] Widyatama A, Venter M, Orejon D, Sefiane K 2023 *Int. J. Thermal Sci* **189** 108238
[10] Barber J, Brutin D, Sefiane K, Tadrist L 2010 *Exp. Therm. Fluid Sci* **34(8)** 1375-88
[11] Wang Y, Sefiane K 2012 *Int. J. Heat Mass Transfer* **55(9-10)** 2235-43
[12] Vermaak M, Orejon D, Dirker J, Sefiane K, Meyer J P 2023 *Appl. Thermal. Eng.* **218** 119292
[13] Lee P S, Garimella S V 2008 *Int. J. Heat Mass Transfer* **51(3-4)** 789-806
[14] Taylor J R 1997 ASMSU/Spartans.4.Spartans Textbook, University Science Books
[15] Vasileiadou P, Sefiane K, Karayiannis T G, Christy J R E 2017 *Appl. Thermal. Eng* **127** 1617-26